NLEFT calculations of nuclei near the dripline

Shuang Zhang

Nuclear Lattice EFT Collaboration

Contents

Background

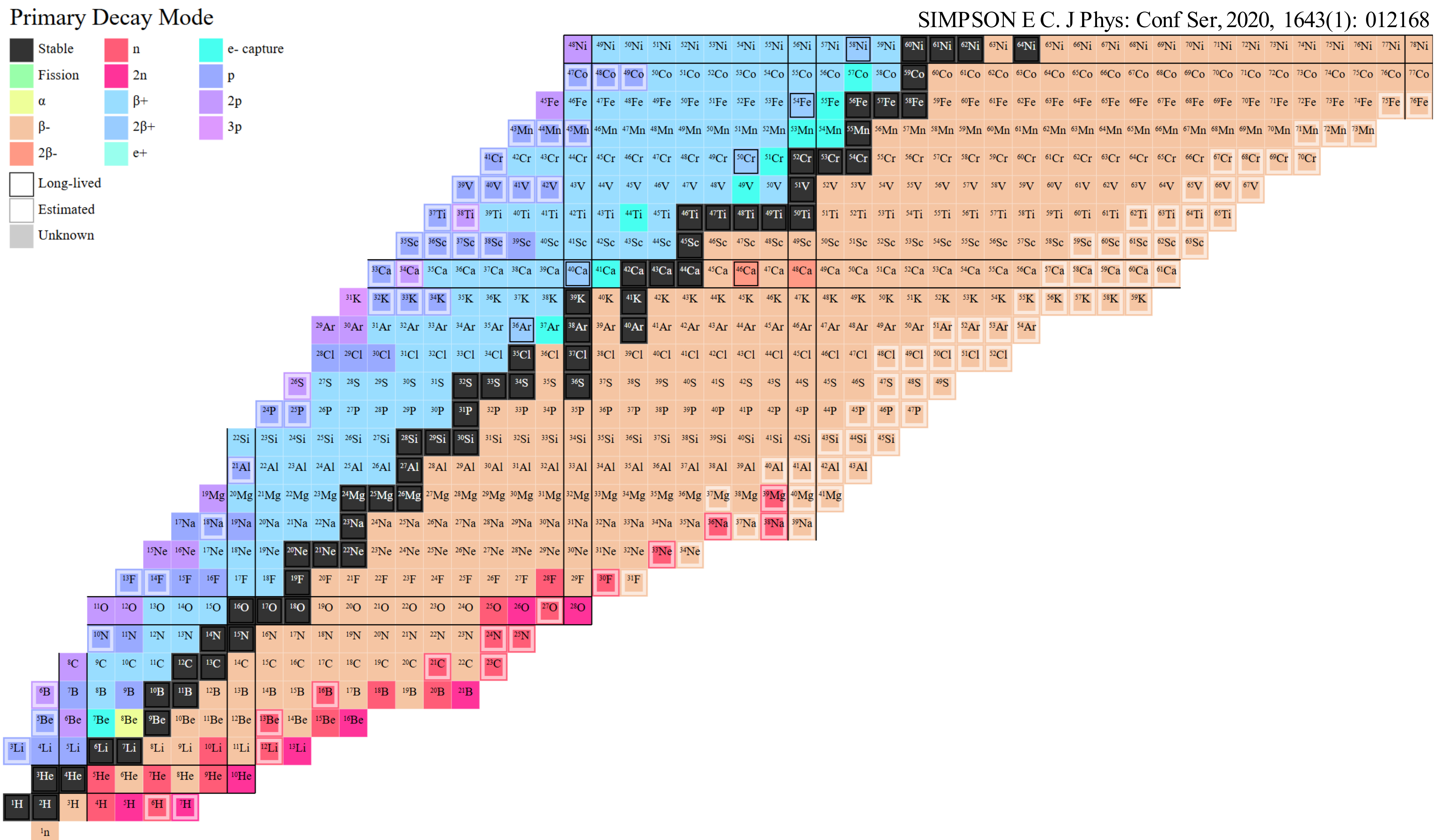
Primary Decay Mode
Stable
Fission
α
β-
2β-
n
2n
β+
2β+
e+
e- capture
p
2p
3p
Long-lived
Estimated
Unknown
SIMPSON E C. J Phys: Conf Ser, 2020, 1643(1): 012168

Background

SIMPSON E C. J Phys: Conf Ser, 2020, 1643(1): 012168

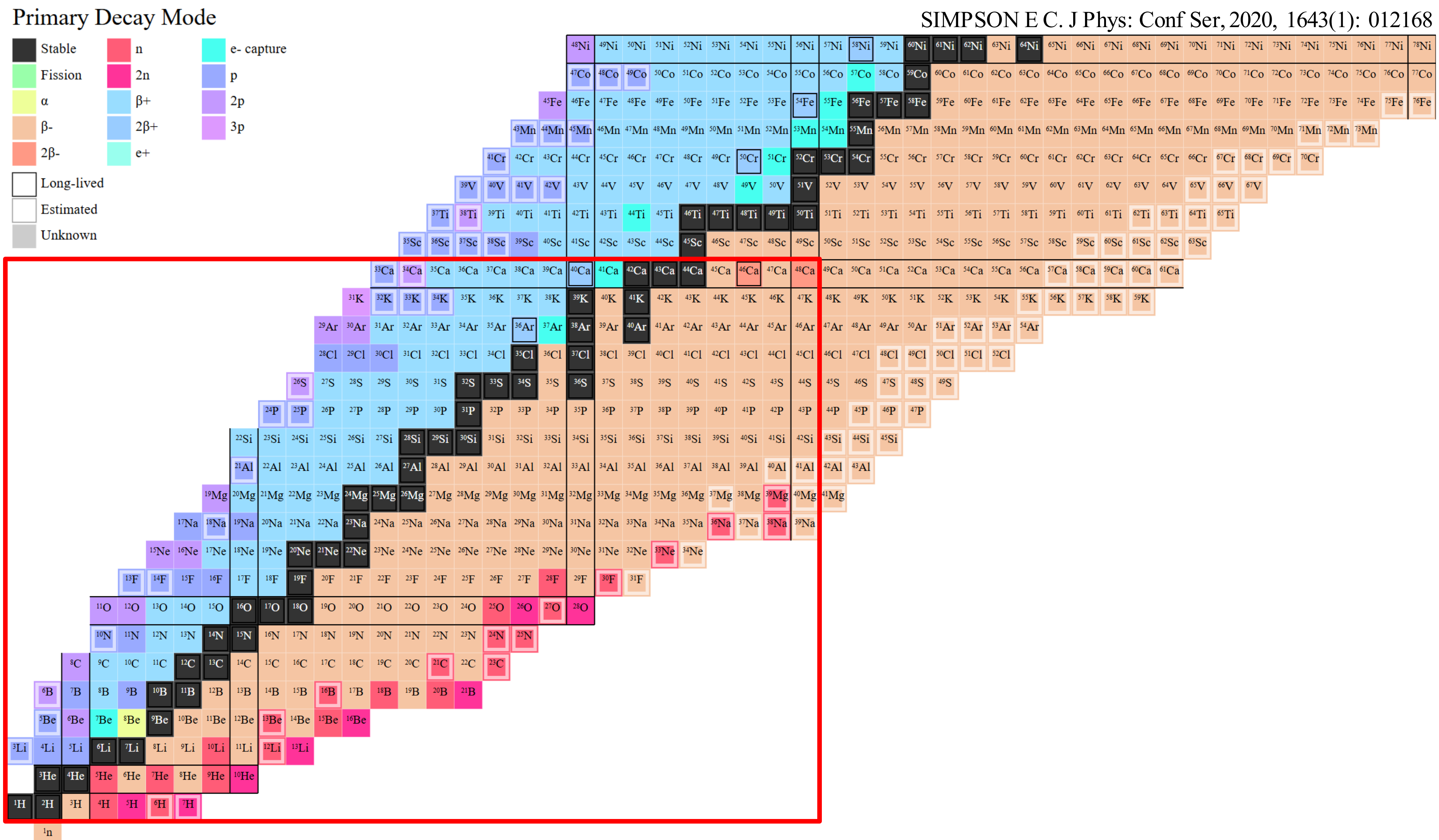

Background

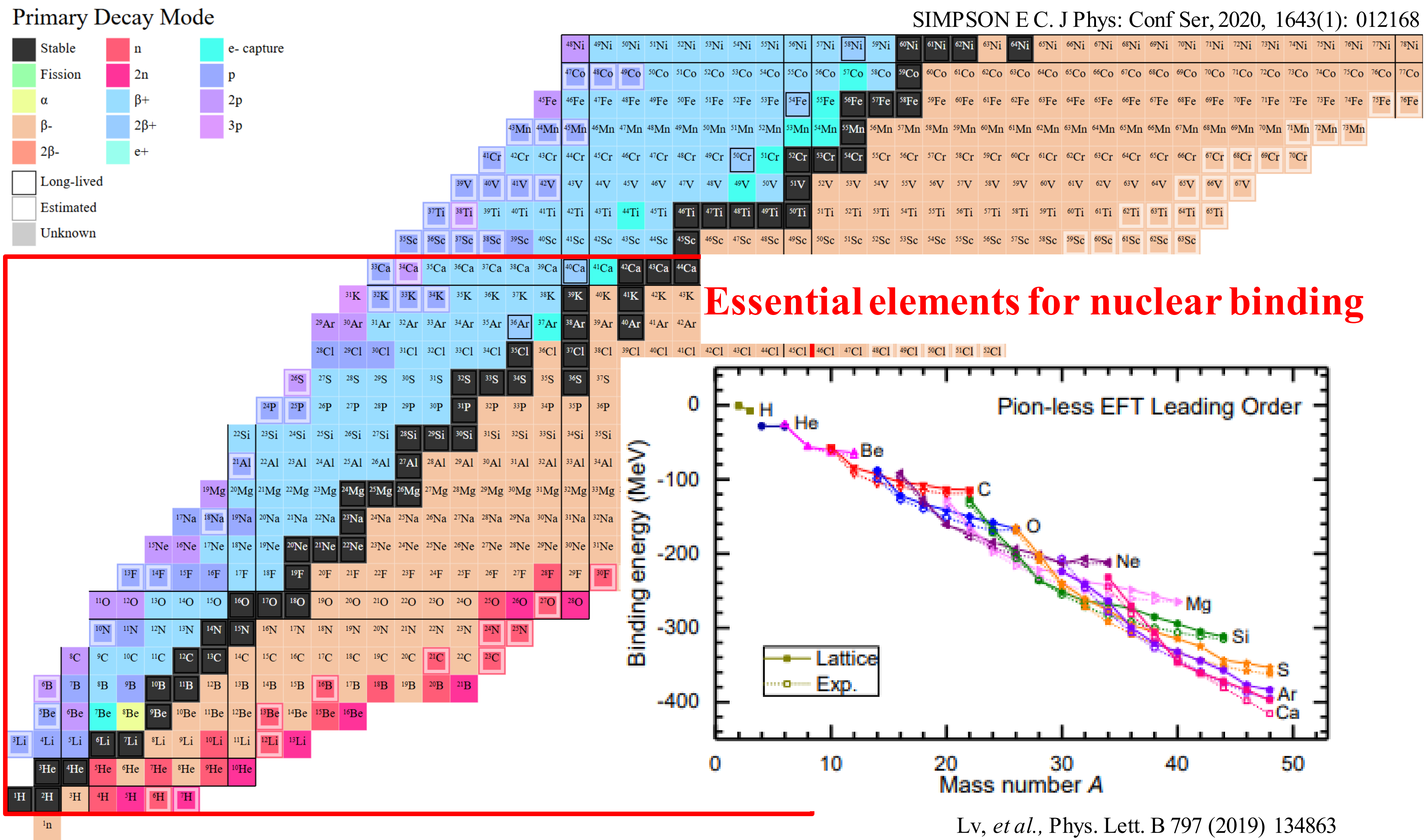

SIMPSON E C. J Phys: Conf Ser, 2020, 1643(1): 012168

Essential elements for nuclear binding

Lv, *et al.*, Phys. Lett. B 797 (2019) 134863

describes binding energies, radii, and the EoS of neutron matter

Background

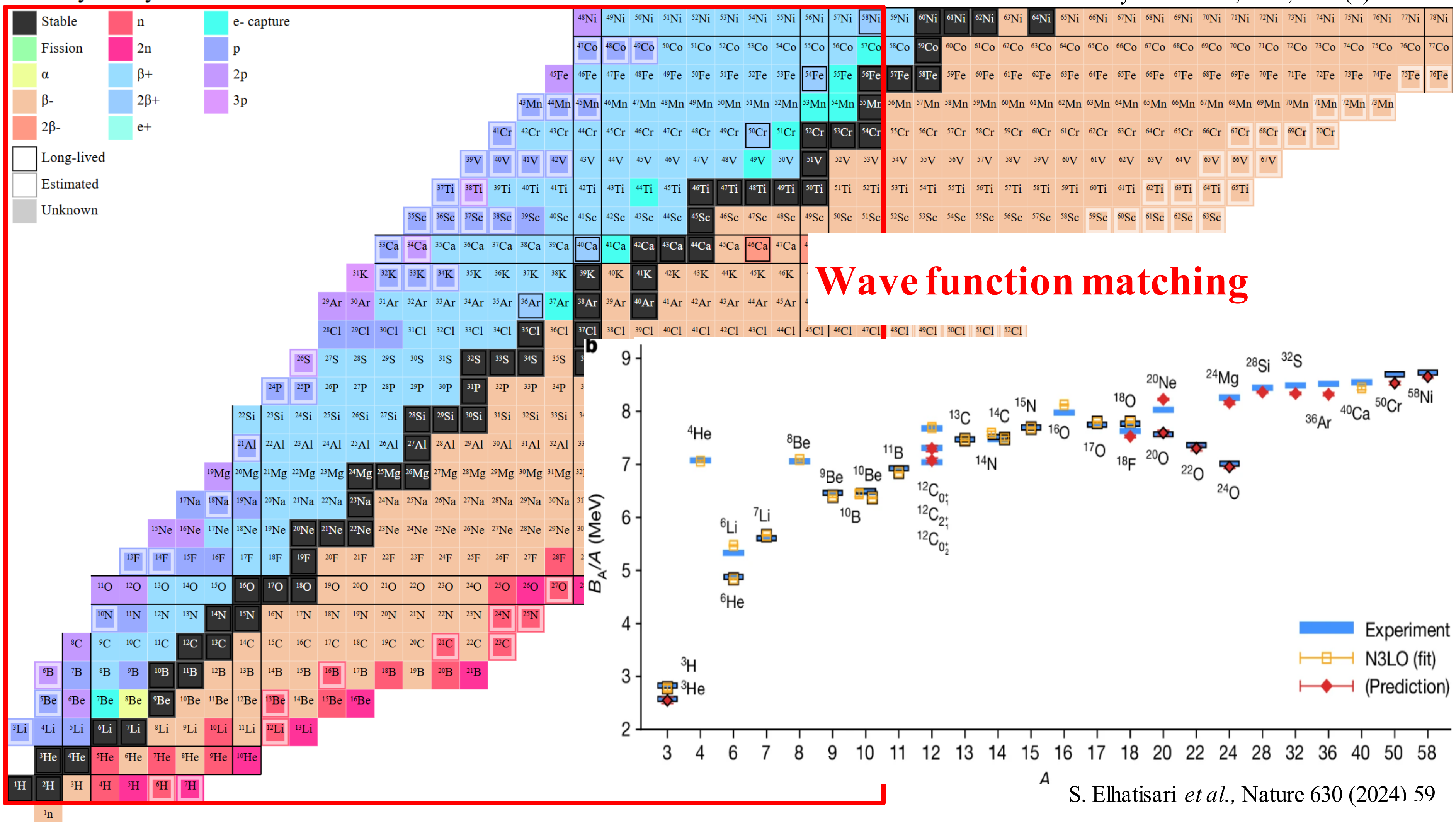

SIMPSON E C. J Phys: Conf Ser, 2020, 1643(1): 012168

Wave function matching

S. Elhatisari *et al.*, Nature 630 (2024) 59

Precisely describes binding energies, radii, and nuclear-matter saturation at N^{3}LO

Background

SIMPSON E C. J Phys: Conf Ser, 2020, 1643(1): 012168

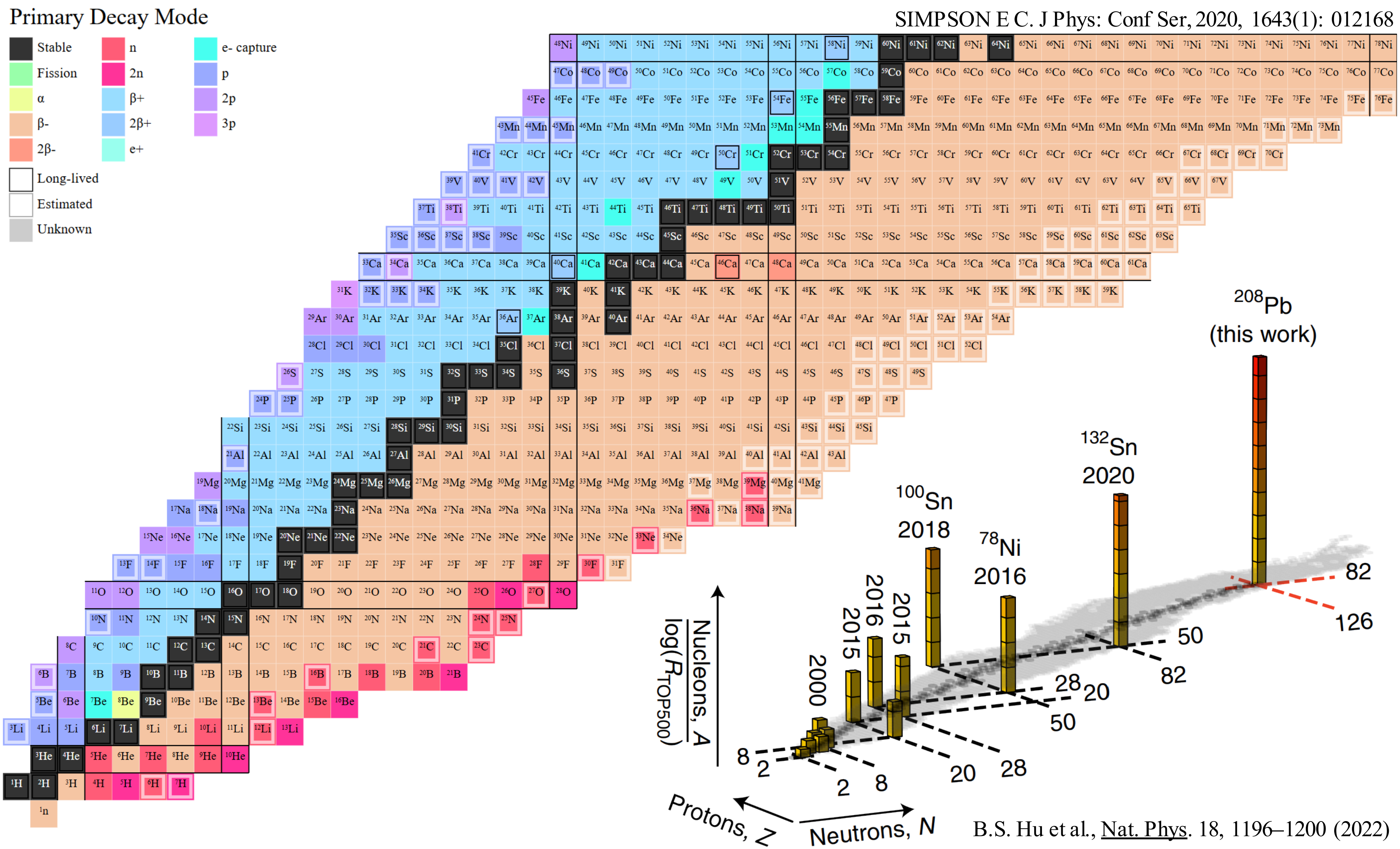

B.S. Hu et al., Nat. Phys. 18, 1196–1200 (2022)

Background

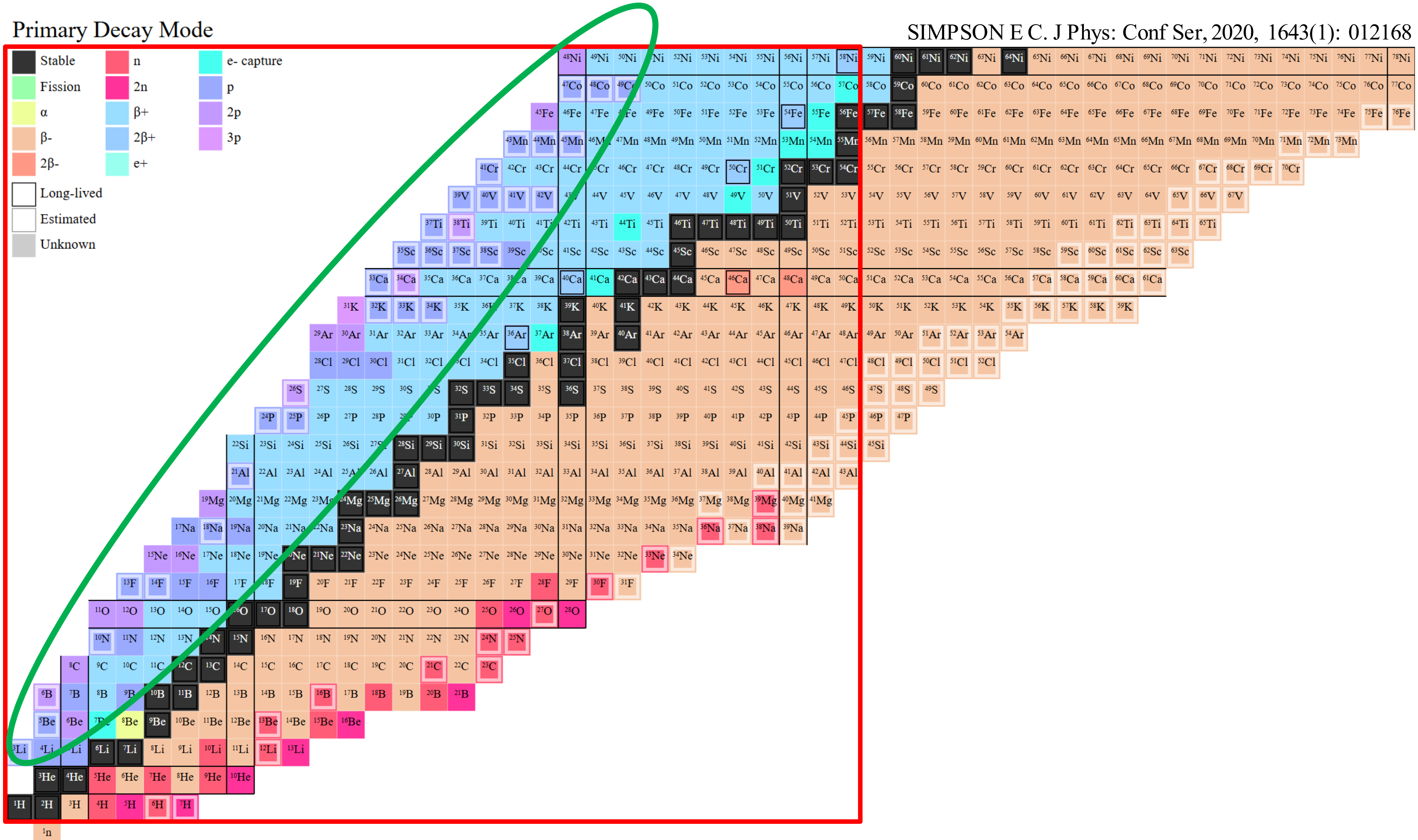

SIMPSON E C. J Phys: Conf Ser, 2020, 1643(1): 012168

Background

SIMPSON E C. J Phys: Conf Ser, 2020, 1643(1): 012168

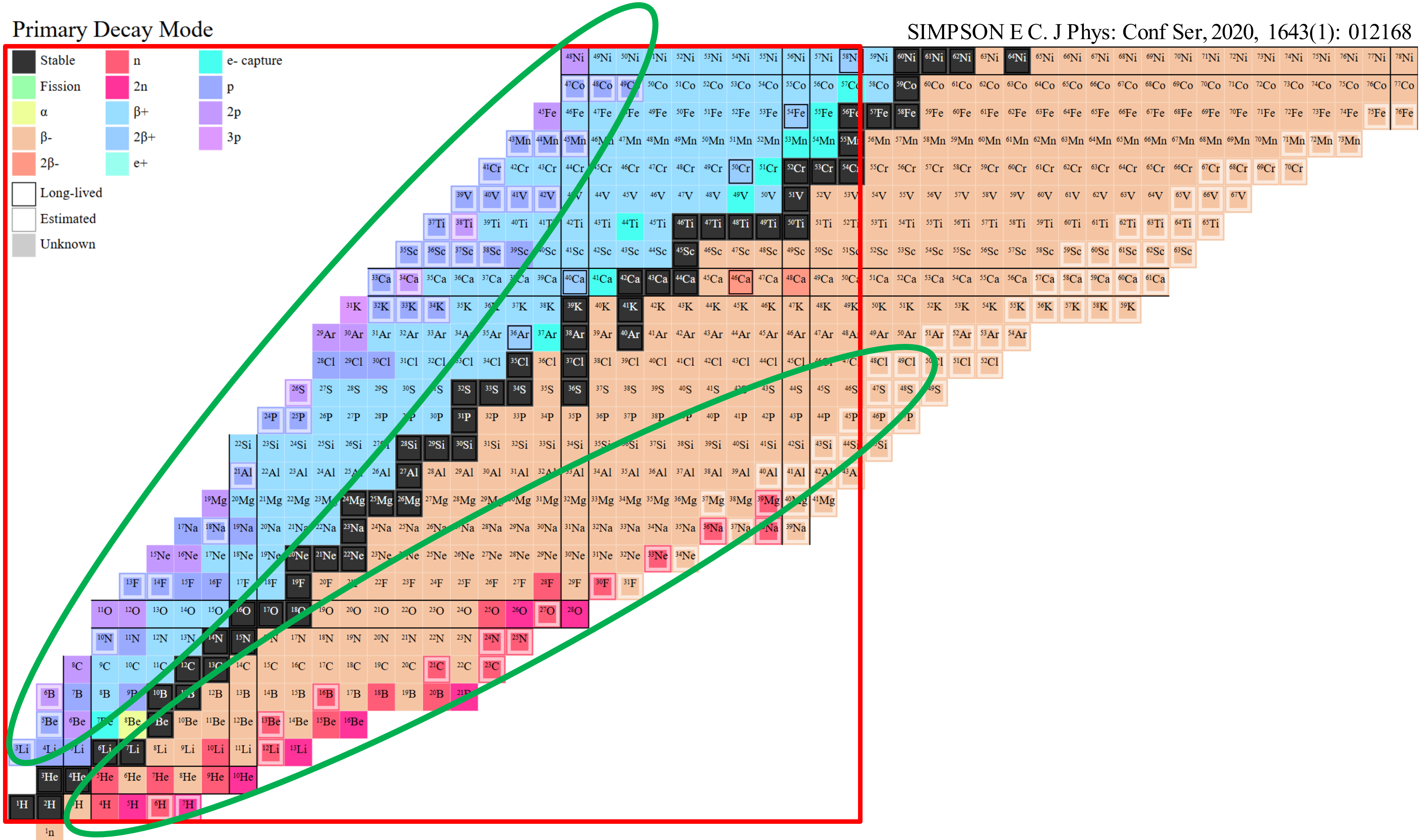

Background

Primary Decay Mode

SIMPSON E C. J Phys: Conf Ser, 2020, 1643(1): 012168

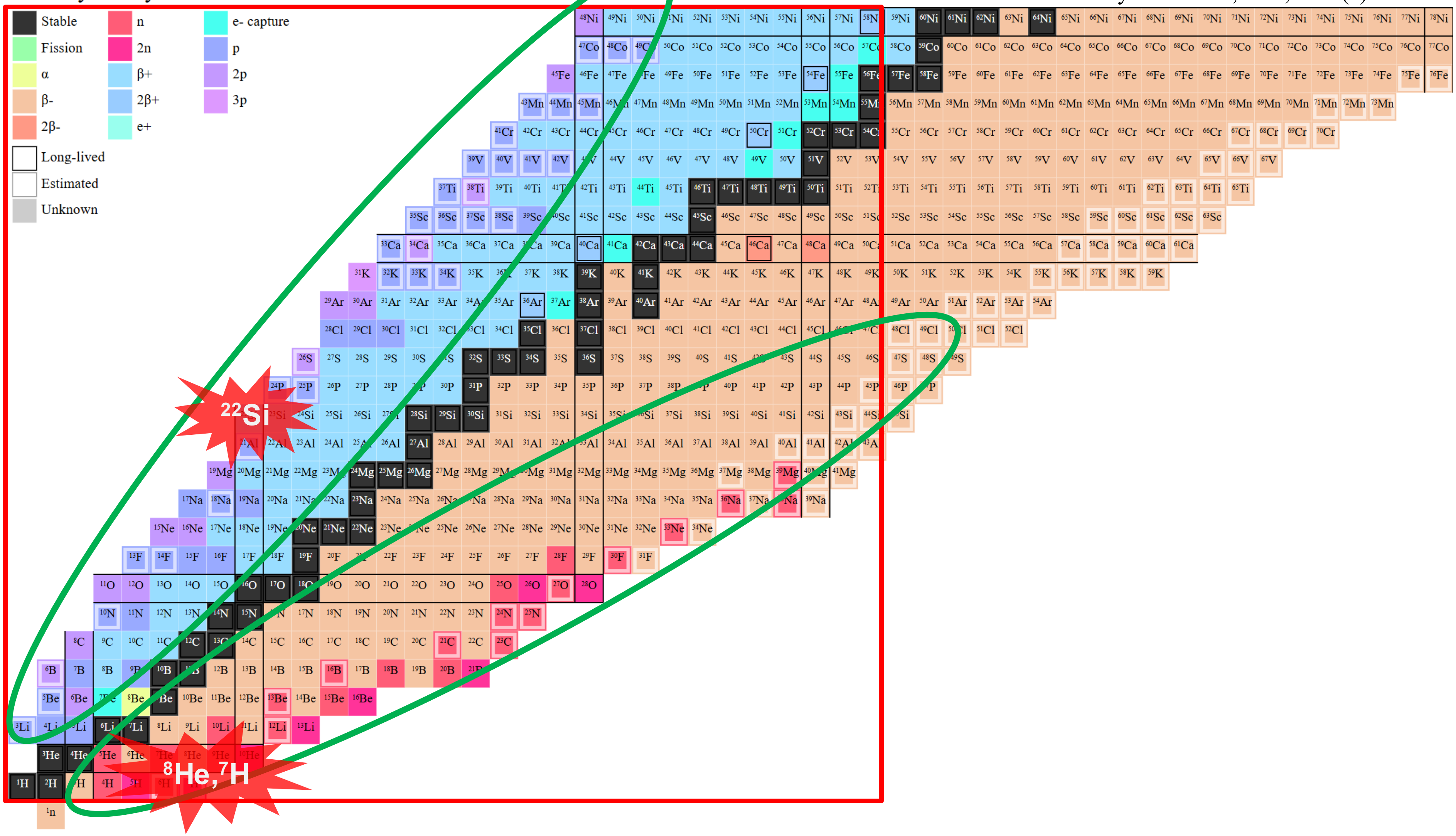

NLEFT framework

■ Chiral force

Discretized in lattice space
a ~ 1.32 fm
np phase shifts to N^{3}LO

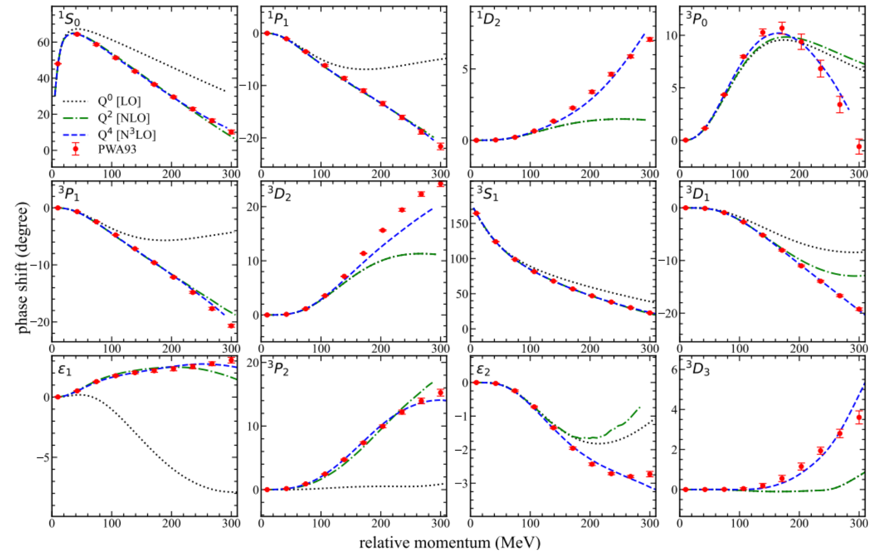

S. Elhatisari *et al.*, Nature 630 (2024) 59
Li *et al.*, Phys. Rev. C 98 (2018) 044002; Phys. Rev. C 99 (2019) 064001

■ Many-body method

Auxiliary field Quantum Monte Carlo

Full sets of many–body correlations
Get states from imaginary time projection

$$|\Psi_{g.s.}\rangle \propto \lim_{\tau\to\infty} \exp(-\tau H)\,|\Psi_A\rangle$$

Wave function Matching

H_S (contact, regularized OPE)
Mapping the unitarily transformed H'_x to H_S

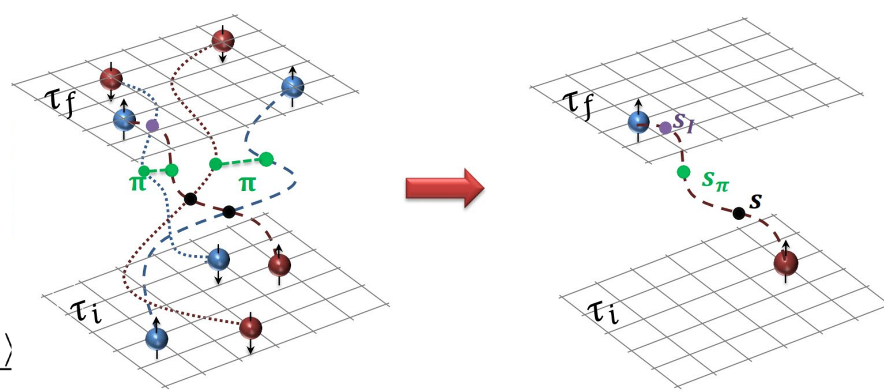

Perturbative method in QMC

$$\langle\mathcal{O}\rangle = \frac{\langle\Psi|\mathcal{O}|\Psi\rangle}{\langle\Psi|\Psi\rangle} = \frac{\langle\Psi^{(0)}+\Psi^{(1)}+\cdots|\mathcal{O}|\Psi^{(0)}+\Psi^{(1)}+\cdots\rangle}{\langle\Psi^{(0)}+\Psi^{(1)}+\cdots|\Psi^{(0)}+\Psi^{(1)}+\cdots\rangle}$$

Lv *et al.*, Phys. Lett. B 797 (2019) 134863; Phys. Rev. Lett. 128, 242501 (2022)

Pinhole method

$$p = \frac{|\langle \Psi_f | M(s_{L_t}) \cdots M(s_{L_t/2+1}) \rho_{i_A, j_A}(\mathbf{n}_A) M(s_{L_t/2}) \cdots M(s_1) | \Psi_i \rangle|}{\sum |\langle \Psi_f | M(s_{L_t}) \cdots M(s_{L_t/2+1}) \rho_{i_A, j_A}(\mathbf{n}_A) M(s_{L_t/2}) \cdots M(s_1) | \Psi_i \rangle|}$$

$$\langle \Psi_j | \; M(s_{L_t}) \cdots M(s_{L_t/2+1}) \cdots \quad \cdots M(s_{L_t}/2) \cdots M(s_1) \; | \Psi_i \rangle$$

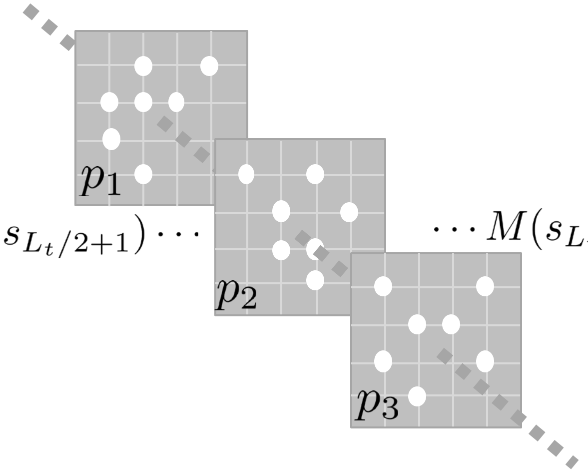

Coordinate space

Insert A-body density operator
sample |r,i,j>
Translation e^{iPRn}|r> orth.|r>
No rotational invariance (irrep projection)

Configuration space

Insert A-body HO basis in m-scheme
sample |*nljm*> with constraints on P_{tot} and M_{tot}
Spherical basis
Breaks translational invariance

S. Elhatisari *et al.*, Phys. Rev. Lett. **119**, 222505, S. Zhang *et al.*, arXiv:2411.17462

Combining density correlations with any observable of physical interest, we are able to probe the underlying structure of the nuclei.

Why ^{22}Si?

Doubly closed shell nucleus at the dripline

Shell closure in competition with proximity to the dripline

- Mass measurement of ^{22}Al suggested a halo structure
- Isospin asymmetry in the ^{22}Si/^{22}O Gamow-Teller transition
- ΔR_{ch} of $^{36\text{-}38}$Ca impacted by nuclear superfluidity and weak binding

S. E. Campbell *et al.,* PRL 132, 152501 (2024), J. Lee *et al.,* PRL 125, 192503 (2020), A. J. Miller *et al.,* Nat. Phys. 15, 432–436 (2019)

Mass, excited states, radii yet to be determined

- High-precision mass measurement at IMP (ongoing)
- Invariant mass of excited states at FRIB (ongoing)
- Radii? $\Delta R_{ch} \propto |N - Z| \times L$ imposes constraint on the slope L of the symmetry energy

K. König *et al.,* Phys. Rev. Lett. 132, 162502 (2024)

Theoretical studies

- Diverse S_{2p} predictions from various many-body methods

Why ^{22}Si?

Doubly closed shell nucleus at the dripline

^{22}Si	method	S_{2p}	notes
	EXP[1]	645(100) keV	weakly bound, indirect experimental measurement **M. Babo, Thesis, Université de Caen Normandie (2016)**
	EXP[2]	-108(125) keV	weakly unbound, indirect experimental measurement **X.X. Xu, et al., PLB 766, 312 (2017)**
	MBPT	-120 keV	2-p emission candidates, chiral NN+3N, $sdp_{3/2}f_{7/2}$ **J.D. Holt, et al., PRL 110, 022502 (2013)**
	IMSRG	-382 keV∼ -558 keV	weakly unbound, EM1.8/2.0, different valence spaces **S.R. Stroberg, et al., PRL 126, 022501 (2017)**
	GSM	674 keV	weakly bound, chiral NN+3N, $sdp_{3/2}f_{7/2}$ **S. Zhang, et al., PLB 827, 136958 (2022)**

Table 1: Current status of experimental and theoretical study on ^{22}Si

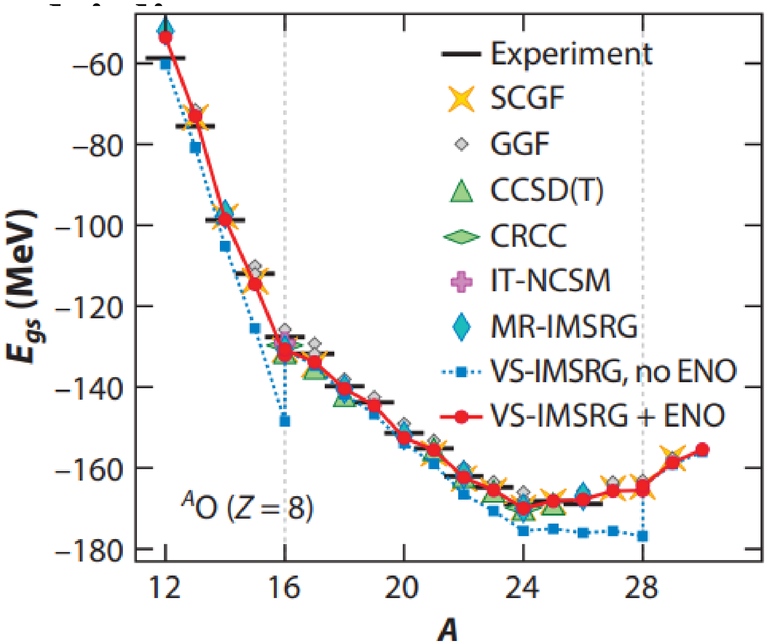

S. R. Stroberg, *et al.,* Annu. Rev. Nucl. Part. Sci. 69, 307 (2019), 1902.06154

Theoretical studies

- Diverse S_{2p} predictions from various many-body methods

Why ^{22}Si?

Doubly closed shell nucleus at the dripline

^{22}Si method	S_{2p}	notes
EXP[1]	645(100) keV	weakly bound, indirect experimental measurement M. Babo, Thesis, Université de Caen Normandie (2016)
EXP[2]	-108(125) keV	weakly unbound, indirect experimental measurement X.X. Xu, et al., PLB 766, 312 (2017)
MBPT	-120 keV	2-p emission candidates, chiral NN+3N, $sdp_{3/2}f_{7/2}$ J.D. Holt, et al., PRL 110, 022502 (2013)
IMSRG	-382 keV∼ -558 keV	weakly unbound, EM1.8/2.0, different valence spaces S.R. Stroberg, et al., PRL 126, 022501 (2017)
GSM	674 keV	weakly bound, chiral NN+3N, $sdp_{3/2}f_{7/2}$ S. Zhang, et al., PLB 827, 136958 (2022)

Table 1: Current status of experimental and theoretical study on ^{22}Si

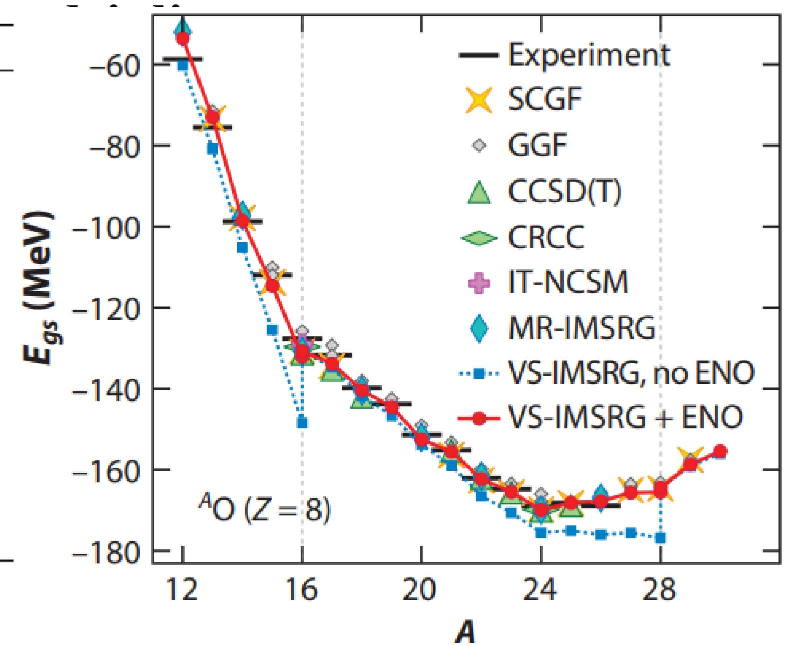

S. R. Stroberg, *et al.*, Annu. Rev. Nucl. Part. Sci. 69, 307 (2019), 1902.06154

Theoretical studies

- Diverse S_{2p} predictions from various many-body methods

- 2+ states evolution insufficient to determine the $N = 8$ shell closure — J. G. Li *et al.*, PLB 846, 138197 (2023)
- Charge radii questions magicity at $N = 32$ of Ca and K isotopes — A. Koszorús, et al. Nat. Phys. 17, 439–443 (2021)

F. Wienholtz *et al.*, Nature 498, 346–349 (2013), R. F. Garcia Ruiz *et al.*, Nat. Phys. 12,594–598 (2016)

Explore this question from the perspective of nucleon distributions in ^{22}Si

Energy

S. Zhang *et al.*, arXiv:2411.17462

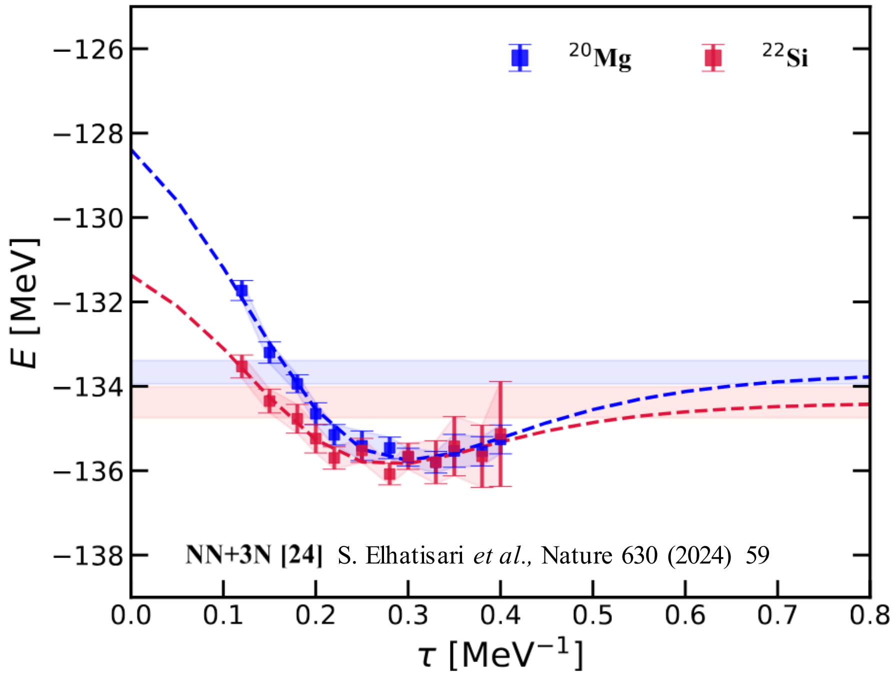

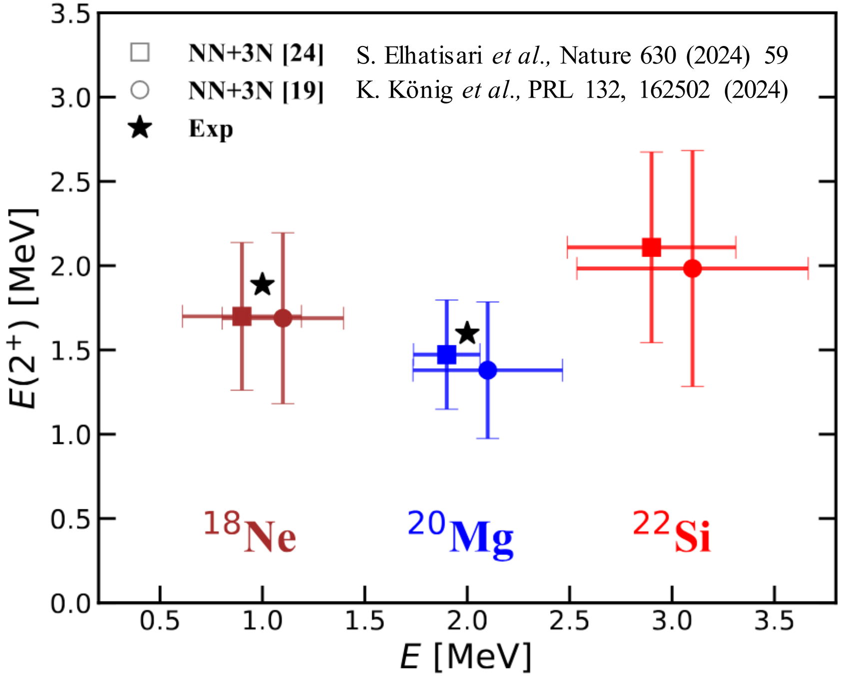

	$E_{g.s.}[^{22}\mathrm{Si}]$	$E_{g.s.}[^{20}\mathrm{Mg}]$	S_{2p}
H_χ[24]	-134.38 (39)	-133.66 (28)	0.72 (48)
H_χ[19]	-136.28 (41)	-134.94 (18)	1.34 (45)
EXP		-134.61	

	$E_{2+}[^{22}\mathrm{Si}]$	$E_{2+}[^{20}\mathrm{Mg}]$	$E_{2+}[^{18}\mathrm{Ne}]$
H_χ[24]	2.11 (57)	1.47 (32)	1.70 (44)
H_χ[19]	1.98 (70)	1.38 (40)	1.69 (51)
EXP		1.60	1.89

τ from 0.3 MeV^{-1} to 0.4 MeV^{-1}

g.s. energies change by less than 0.36 MeV
^{22}Si consistently more bound than ^{20}Mg

Suggest a possible *Z* = 14 subshell closure

Radii

S. Zhang *et al.*, arXiv:2411.17462

	R_{ch}	$\Delta R_{ch}(^{22}\text{Si-}^{20}\text{Mg})$	$\Delta R_{ch}(^{22}\text{Si-}^{22}\text{O})$
H_χ [24]	3.277 (19)	0.070 (31)	0.361 (32)
H_χ [19]	3.196 (17)	0.070 (28)	0.370 (29)

Experiment:

$$\Delta R_{ch}(^{28}\text{Si-}^{26}\text{Mg}) = 0.088 \text{ fm}$$
$$\Delta R_{ch}(^{30}\text{Si-}^{28}\text{Mg}) = 0.064 \text{ fm}$$
$$\Delta R_{ch}(^{32}\text{Si-}^{30}\text{Mg}) = 0.042 \text{ fm}$$

D. T. Yordanov *et al.*, PRL 108, 042504 (2012)
K. König *et al.*, PRL 132, 162502 (2024)

No significantly changes in shell structure from proton-rich to neutron-rich side.

ΔR_{ch} of ^{22}Si-^{22}O show good agreement with two chiral NN+3N forces

Lattice simulations:

Consistent with CC prediction within 3σ confidence
ΔR_{ch} [CC] = 0.429 (21)

Relatively small, a suppression of the slope L?

S. J. Novario *et al.*, PRL 130, 032501 (2023)

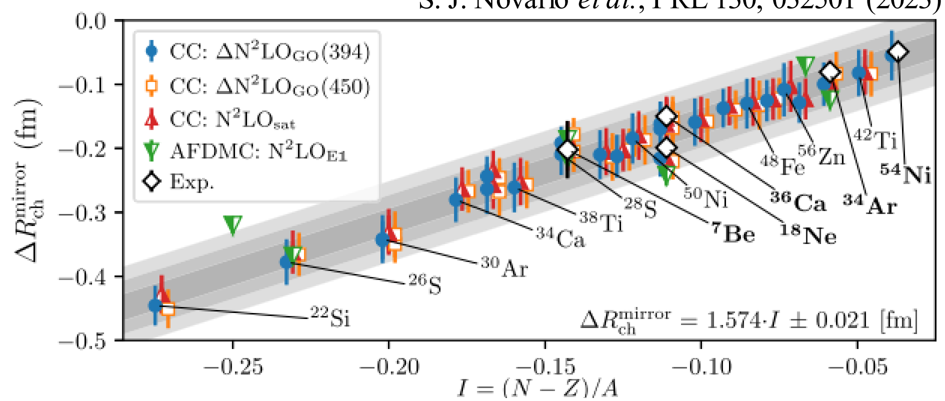

Nucleon distributions

Nucleon ordering operators:

S. Zhang *et al.*, arXiv:2411.17462

$$\hat{\Pi}_i(r) = \delta(r - r_{\hat{\pi}(i)}) \qquad \hat{\pi}(i) = \arg \min_{k \notin \{\pi(1),\ldots,\pi(i-1)\}} \{\hat{r}_k\}$$

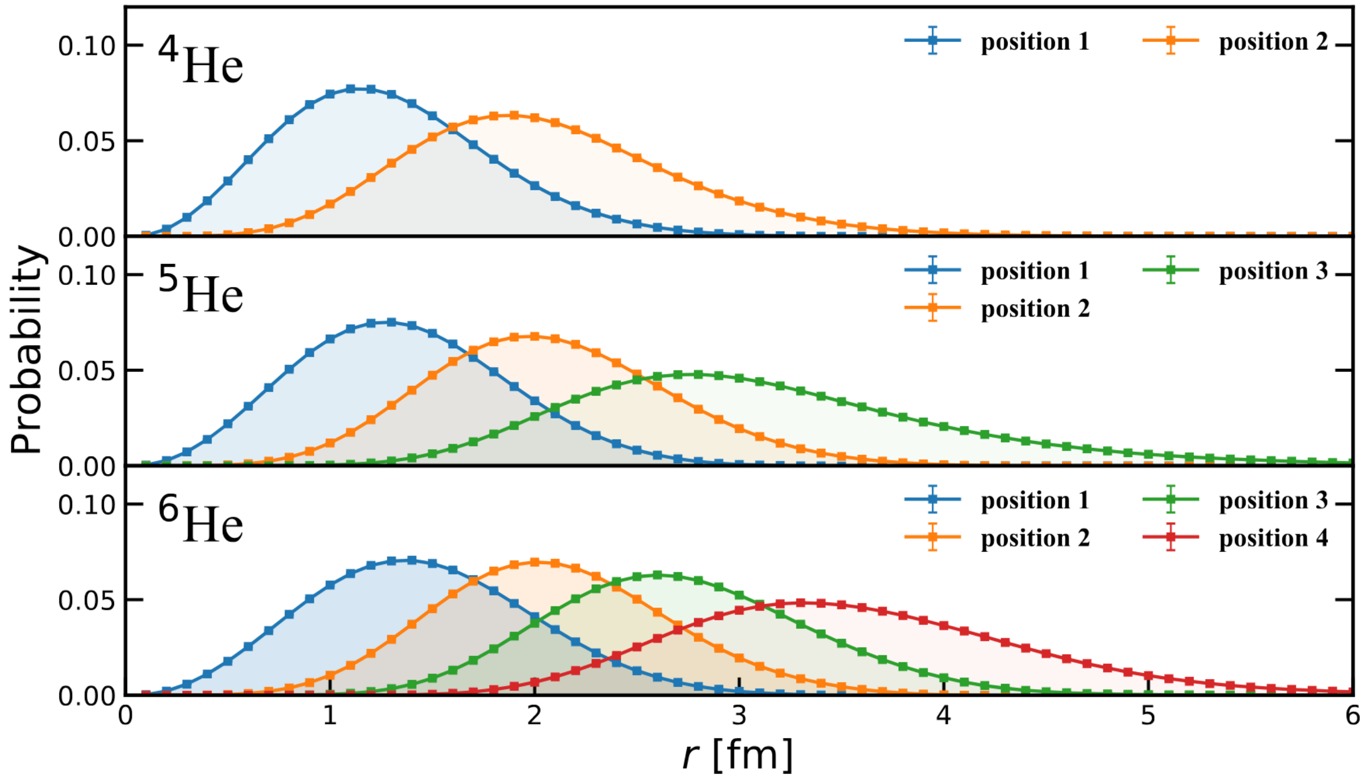

First and second layers of ^{4}He share identical Gaussian widths

^{5}He&^{6}He outer layers exhibit significant spatial extension, unlike inner layers

Reveals arrangement and localization, linking to the shell closure to some extent

Nucleon distributions

Spatial arrangement of protons in the $N = 8$ isotones

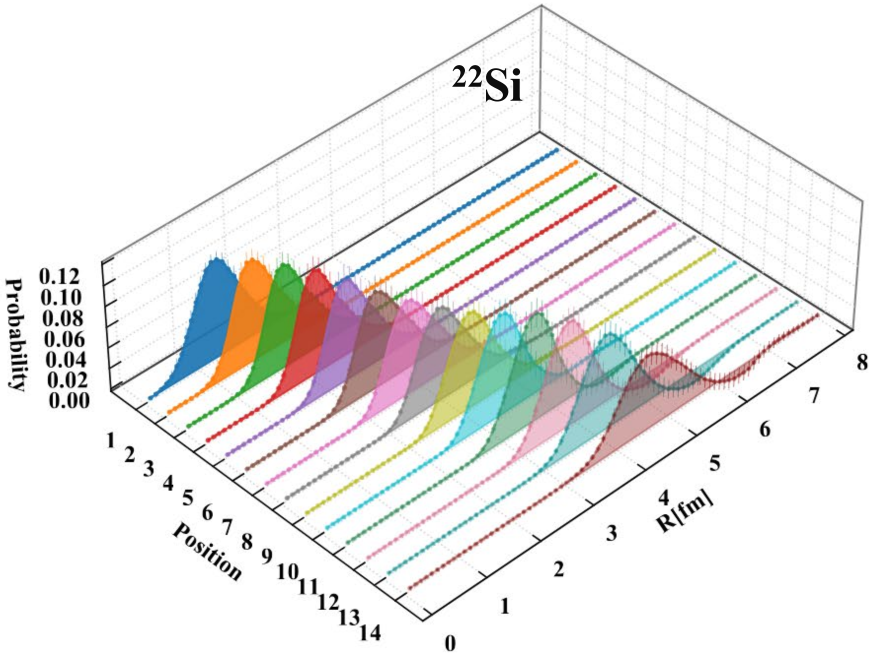

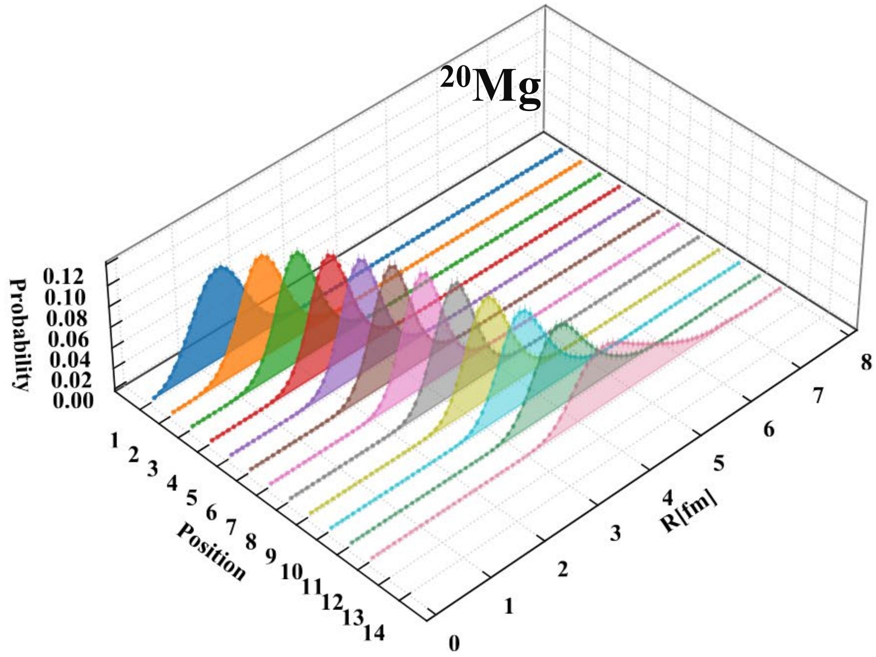

The extra 2*p* in ^{22}Si are likely positioned near the regions corresponding to the 9th and 11th layers

Outer layer in ^{22}Si shows a similar broadening pattern to the inner layers and exhibits spatial localization characteristics

S. Zhang *et al.*, arXiv:2411.17462

Nucleon distributions

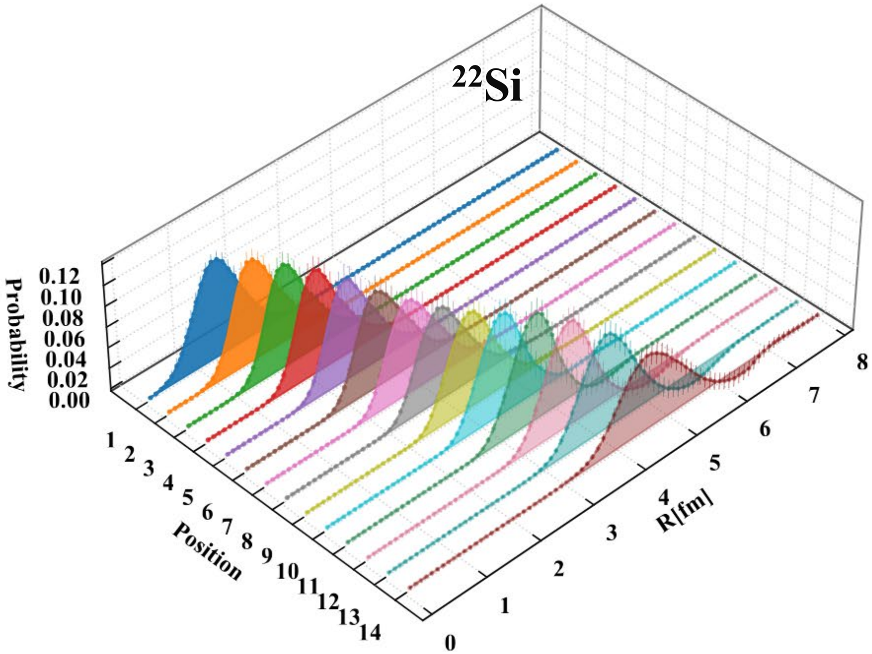

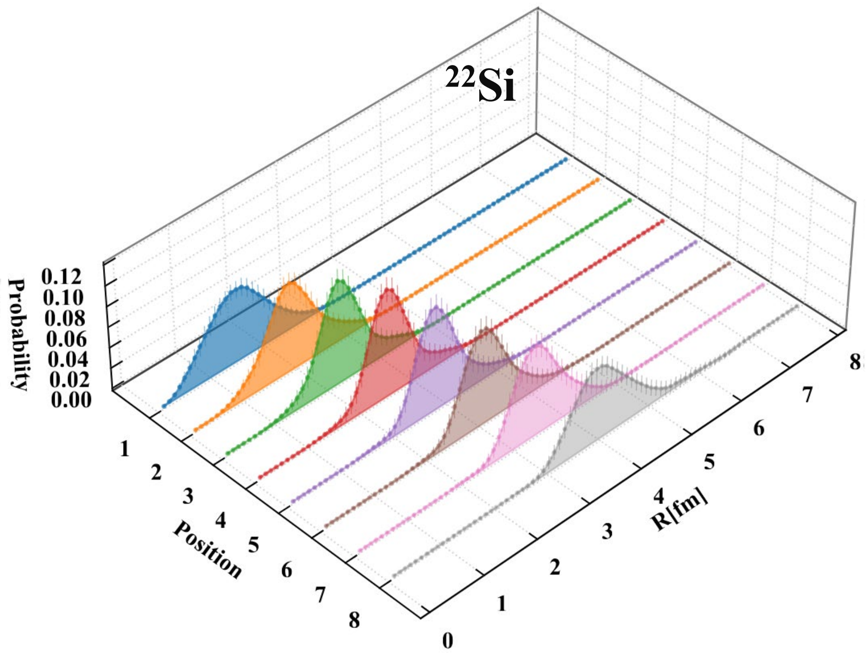

The extra 2*p* in ^{22}Si are likely positioned near the regions corresponding to the 9th and 11th layers

Outer layer in ^{22}Si shows a similar broadening pattern to the inner layers and exhibits spatial localization characteristics

Spatial localizations in Coordinate space linked to shell closure features in SM languages

Presence of shell closure at $Z = 14$ and $N = 8$ in ^{22}Si

S. Zhang *et al.*, arXiv:2411.17462

Occupation numbers via Pinhole method with HO basis

States	$\mathbf{n}_\pi$	$\mathbf{n}_\nu$
$0s_{1/2}[1/2]$	0.935 (132)	1.009 (123)
$0s_{1/2}[-1/2]$	0.970 (135)	0.981 (124)
$0p_{3/2}[3/2]$	0.670 (151)	0.931 (135)
$0p_{3/2}[1/2]$	0.965 (164)	0.805 (123)
$0p_{3/2}[-1/2]$	0.945 (155)	0.901 (139)
$0p_{3/2}[-3/2]$	0.751 (148)	0.911 (137)
$0p_{1/2}[1/2]$	0.901 (131)	0.877 (135)
$0p_{1/2}[-1/2]$	1.049 (161)	0.938 (147)
$0d_{5/2}[5/2]$	1.018 (205)	
$0d_{5/2}[3/2]$	1.056 (229)	
$0d_{5/2}[1/2]$	0.980 (217)	
$0d_{5/2}[-1/2]$	1.106 (223)	
$0d_{5/2}[-3/2]$	0.875 (209)	
$0d_{5/2}[-5/2]$	1.063 (204)	
$1s_{1/2}[1/2]$	0.141 (173)	
$1s_{1/2}[-1/2]$	0.160 (150)	
$0d_{3/2}[3/2]$	−0.127 (169)	
$0d_{3/2}[1/2]$	−0.003 (162)	
$0d_{3/2}[-1/2]$	0.202 (156)	
$0d_{3/2}[-3/2]$	0.145 (143)	

Occupation number <<1 → particle-hole excitations

$0p$ orbitals of proton:

$0p_{3/2}[\ 3/2] = 0.979$ (6) with H_s
$0p_{3/2}[-3/2] = 0.982$ (7) with H_s
fully occupied w/o perturbation corrections

Outer $0d_{5/2}$ orbitals:

fully occupied → suggests limited particle-hole excitation

Statistical Considerations:

Lower-than-expected occupation for $0p_{3/2}$
negative value for $0d_{3/2}[3/2]$
Sign problem with N^3LO & Insufficient statistics due to full many-body correlations

Upper limits considering errors:

$0p_{3/2}[\ 3/2] \leq 0.821$
$0p_{3/2}[-3/2] \leq 0.899$
$0d_{3/2}[\ 3/2] \sim 0$

Occupation numbers via Pinhole method with HO basis

States	n_π	n_ν
$0s_{1/2}[1/2]$	0.935 (132)	1.009 (123)
$0s_{1/2}[-1/2]$	0.970 (135)	0.981 (124)
$0p_{3/2}[3/2]$	0.670 (151)	0.931 (135)
$0p_{3/2}[1/2]$	0.965 (164)	0.805 (123)
$0p_{3/2}[-1/2]$	0.945 (155)	0.901 (139)
$0p_{3/2}[-3/2]$	0.751 (148)	0.911 (137)
$0p_{1/2}[1/2]$	0.901 (131)	0.877 (135)
$0p_{1/2}[-1/2]$	1.049 (161)	0.938 (147)
$0d_{5/2}[5/2]$	1.018 (205)	
$0d_{5/2}[3/2]$	1.056 (229)	
$0d_{5/2}[1/2]$	0.980 (217)	
$0d_{5/2}[-1/2]$	1.106 (223)	
$0d_{5/2}[-3/2]$	0.875 (209)	
$0d_{5/2}[-5/2]$	1.063 (204)	
$1s_{1/2}[1/2]$	0.141 (173)	
$1s_{1/2}[-1/2]$	0.160 (150)	
$0d_{3/2}[3/2]$	−0.127 (169)	
$0d_{3/2}[1/2]$	−0.003 (162)	
$0d_{3/2}[-1/2]$	0.202 (156)	
$0d_{3/2}[-3/2]$	0.145 (143)	

Occupation number <<1 → particle-hole excitations

$0p$ orbitals of proton:

$0p_{3/2}[\ 3/2] = 0.979$ (6) with H_s
$0p_{3/2}[-3/2] = 0.982$ (7) with H_s
fully occupied w/o perturbation corrections

Outer $0d_{5/2}$ orbitals:

fully occupied → suggests limited particle-hole excitation

Statistical Considerations:

Lower-than-expected occupation for $0p_{3/2}$
negative value for $0d_{3/2}[3/2]$
Sign problem with N^3LO & Insufficient statistics due to full many-body correlations

Upper limits considering errors:

$0p_{3/2}[\ 3/2] \leq 0.821$
$0p_{3/2}[-3/2] \leq 0.899$
$0d_{3/2}[\ 3/2] \sim 0$

Occu. numbers support the existence of shell closure (as indicated by the 2^+ and spatial localizations) rather than a genuine destruction of the shell closure

Providing pathways for future comparisons with configuration space many-body methods

S. Zhang *et al.*, arXiv:2411.17462

nn correlations in light nuclei

Observation of 0_2^+ in ^{8}He with the condensatelike α+2n+2n cluster

E = 6.66 (6) MeV

M(IS0) = $11^{+1.8}_{-2.3}$ fm^2

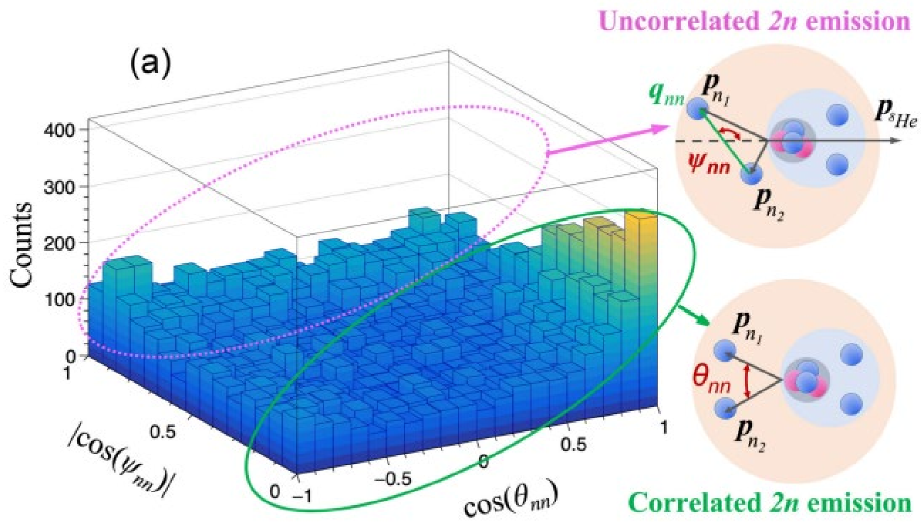

Z. H. Yang, *et. al.*, PhysRevLett.131.242501 (2023)

Green-solid ovals (ψ_{nn} ~ 90°):

Enhancement at θ_{nn} ~ 0°

significant *nn* correlations

Compared to a pure four-neutron system, multi-neutron correlation may be enhanced when 4*n* are weakly bound or unbound around a core.

nn correlations in light nuclei

Uncertainty Analysis:

- Volume Effects: $L = 14$
- Chiral forces: nuclear force parameterizations via history matching

Intrinsic structure

- A-body density with full correlations
- Cluster identification α, 2n, t

Multi-neutron correlations

***nn* correlation analysis**

Three-body systems (Jacobi basis, via pinhole coordinate)

$\alpha + 2n + 2n$

$t + 2n + 2n$

2*n* - 2*n* correlation

Three-body correlation functions:

$\alpha + 2n + 2n$ / $t + 2n + 2n$

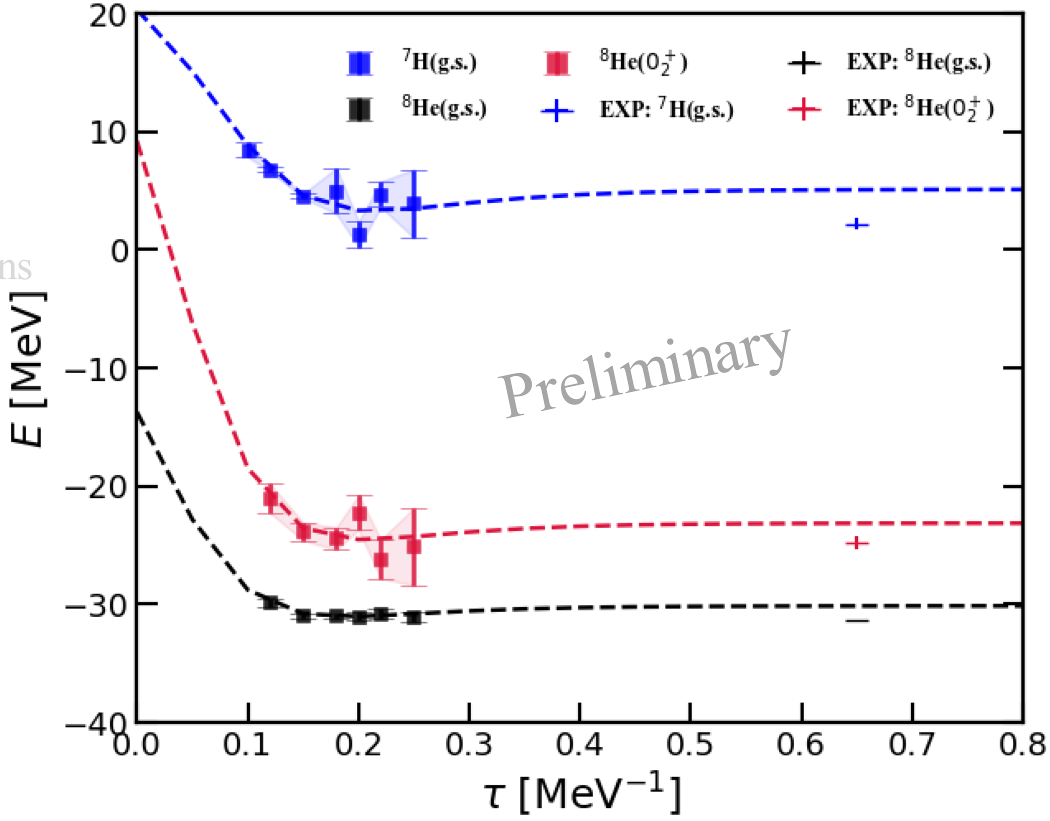

nn correlations in light nuclei

Uncertainty Analysis:

- Volume Effects: $L = 14$
- Chiral forces: nuclear force parameterizations via history matching

Intrinsic structure

- A-body density with full correlations
- Cluster identification α, $2n$, t

Multi-neutron correlations

nn correlation analysis

Three-body systems (Jacobi basis, via pinhole coordinate)

$\alpha + 2n + 2n$

$t + 2n + 2n$

$2n$ - $2n$ correlation

Three-body correlation functions:

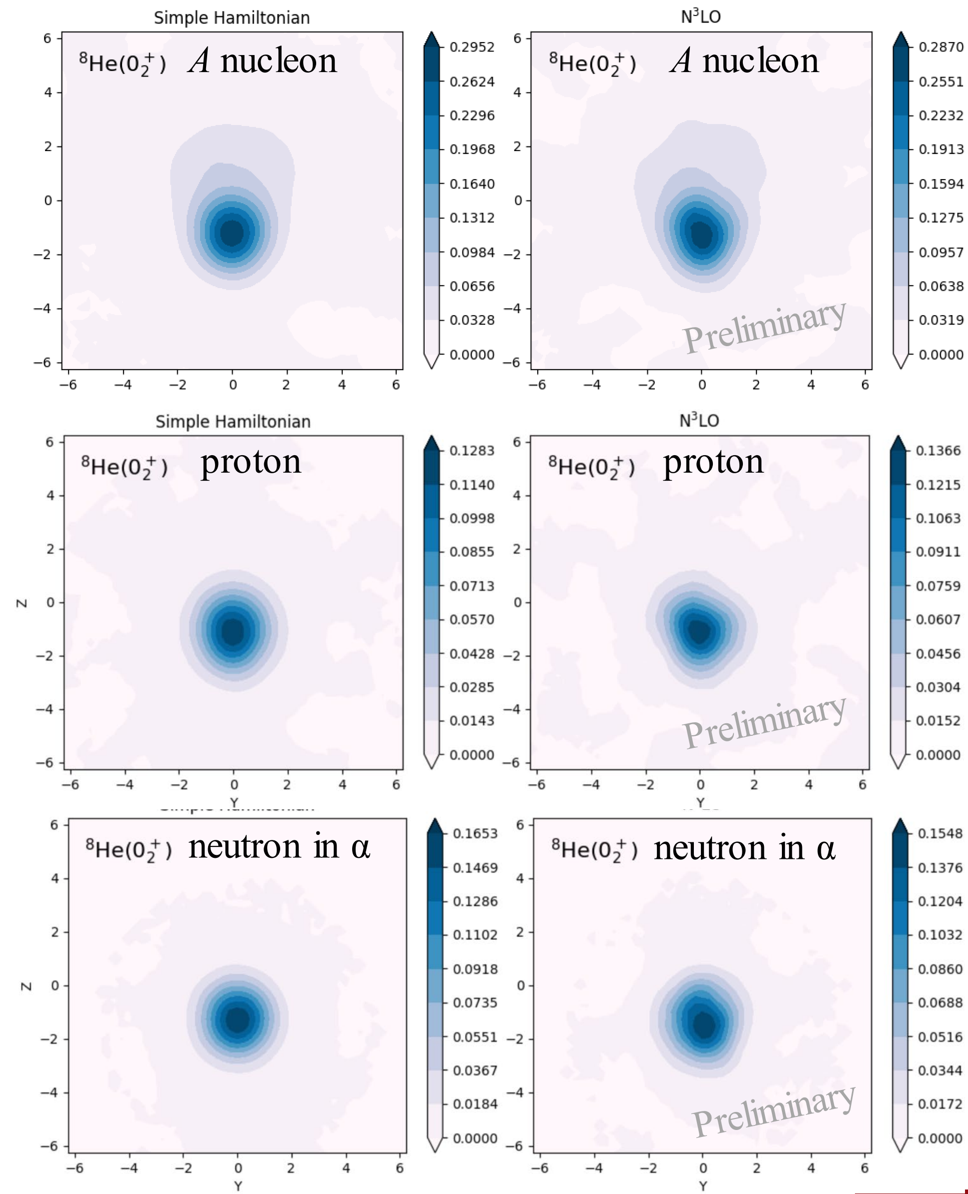

nn correlations in light nuclei

Uncertainty Analysis:

- Volume Effects: $L = 14$
- Chiral forces: nuclear force parameterizations via history matching

Intrinsic structure

- *A*-body density with full correlations
- Cluster identification α, 2*n*, *t*

Multi-neutron correlations

nn correlation analysis

Three-body systems (Jacobi basis, via pinhole coordinate)

α + 2*n* + 2*n*

t + 2*n* + 2*n*

2*n* - 2*n* correlation

Three-body correlation functions:

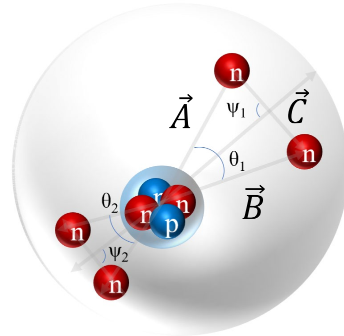

T-type

$\vec{A}$ = n^1(x,y,z) - CoM(x,y,z)

$\vec{B}$ = n^2(x,y,z) - CoM(x,y,z)

$\vec{C}$ = n^1(x,y,z) - n^2(x,y,z)

$$\theta = \frac{\arccos(\vec{A}\cdot\vec{B})}{|\vec{A}||\vec{B}|} \quad \psi = \pi - \theta/2 - \frac{\arccos(\vec{A}\cdot\vec{C})}{|\vec{A}||\vec{C}|}$$

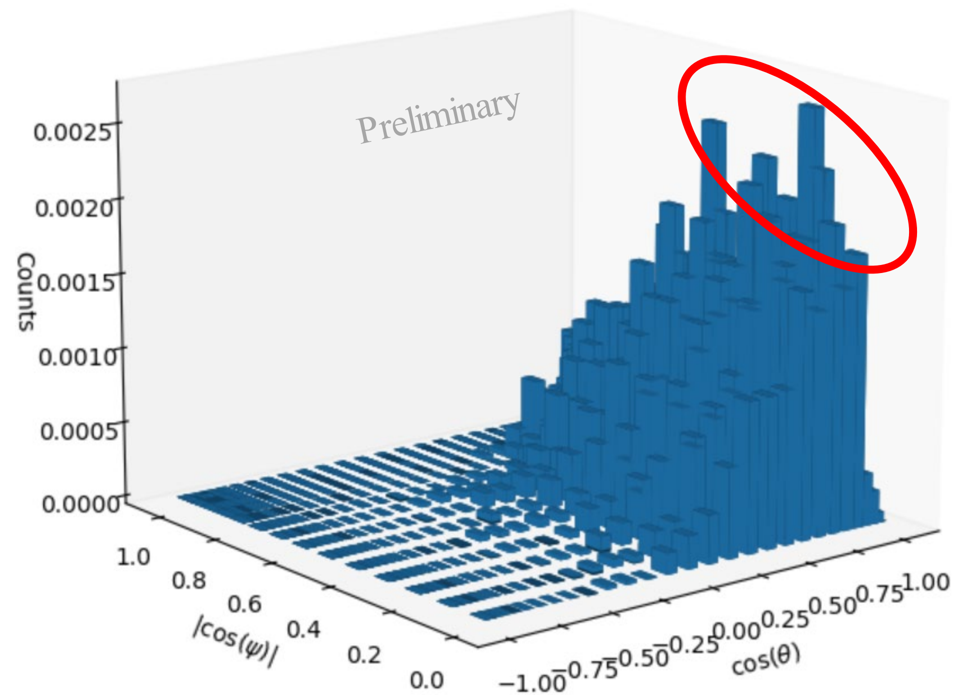

Uncertainty Analysis:

- Volume Effects: $L = 14$
- Chiral forces: nuclear force parameterizations via history matching

Intrinsic structure

- A-body density with full correlations
- Cluster identification α, $2n$, t

Multi-neutron correlations

***nn* correlation analysis**

Three-body systems (Jacobi basis, via pinhole coordinate)

$$\alpha + 2n + 2n$$

$$t + 2n + 2n$$

2*n* - 2*n* correlation

Three-body correlation functions:

$$\rho_3(r_{12}, r_{13}, r_{23}) = \binom{A}{3}\left\langle \prod_{i<j=1}^{3} \delta(|\boldsymbol{r}_i - \boldsymbol{r}_j| - r_{ij}) \right\rangle$$

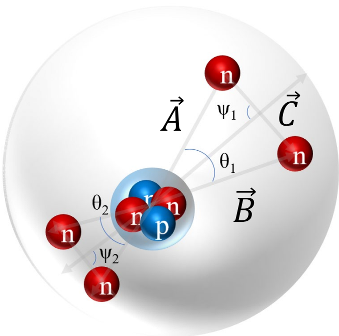

T-type

$\vec{A}$ = $n^1(x,y,z)$ - CoM(x,y,z)
$\vec{B}$ = $n^2(x,y,z)$ - CoM(x,y,z)
$\vec{C}$ = $n^1(x,y,z)$ - $n^2(x,y,z)$

$$\theta = \frac{\arccos(\vec{A}\cdot\vec{B})}{|\vec{A}||\vec{B}|} \quad \psi = \pi - \theta/2 - \frac{\arccos(\vec{A}\cdot\vec{C})}{|\vec{A}||\vec{C}|}$$

If $\theta_1, \theta_2 \sim \mathbf{0}$; $\psi_1, \psi_2 \sim \pi/2$

$d_1(x,y,z) = [n^1(x,y,z) + n^2(x,y,z)]/2$
$d_2(x,y,z) = [n^3(x,y,z) + n^4(x,y,z)]/2$
$\alpha(x,y,z)$

R. Weiss, S. Gandolfi, Phys. Rev. C **108**, L021301

Summary & perspective

□ Proton-rich ^{22}Si

Calculations agree with existing data and predict ^{22}Si as a proton-dripline nucleus, along with its 2^+ state, radius, and spatial properties

Using nucleon ordering operators, we reveal nucleon spatial arrangement and localization, linked to shell closure features

Introducing a novel pinhole method with HO basis, offering new perspectives into a more comprehensive understanding of nuclear structure

□ *nn* correlations in light nuclei

Energies, nucleon density of ^{8}He and ^{7}H

Cluster identification, such as α, 2*n*

□ Further developments

Comparison our ^{22}Si results with upcoming experimental data

Uncertainty quantification in the energies of ^{8}He and ^{7}H, multi-neutron correlations

Extension to heavy nuclei with the benefits of GPU resource

Thank you!